Jürgen Werner, Mingcheng Zhao, Matthias Hillenbrand, Stefan Sinzinger*:*

RBF-based optical surfaces

Zuerst erschienen in:
DGaO-Proceedings. - Erlangen-Nürnberg: Dt. Gesellschaft für angewandte Optik, ISSN 1614-8436. - Bd. 113.2012, P39, insg. 2 S.

URN: urn:nbn:de:0287-2012-P039-2

RBF-based optical surfaces

Jürgen Werner, Mingcheng Zhao, Matthias Hillenbrand, Stefan Sinzinger
Fachgebiet Technische Optik, Technische Universität Ilmenau
mailto:juergen.werner@tu-ilmenau.de

We study the use of radial basis functions (RBF) for describing axially symmetric surfaces in the design of imaging optical systems. Several basis functions as well as the influence of the different parameters are considered.

1 Introduction

Freeform optical surfaces offer additional degrees of freedom for designing imaging systems. This allows for a reduction in the number of optical elements, leading to more compact and lightweight systems, while at the same time improving the image quality. Radial basis functions have been used for many years in function approximation and might be a suitable form to represent freeform optical surfaces. Cakmakci et al. used RBFs to design mirrors for head-worn displays [1]. Brenner [2] and Ettl et al. [3] used RBFs for surface approximation and surface reconstruction. We investigate basic properties of axially symmetric surfaces composed of one-dimensional RBFs as a first step towards freeform RBF surfaces. The surfaces are implemented as a user defined DLL for Zemax.

2 Definition

We define a RBF surface by

$$z(r) = \tilde{z}(r) - \tilde{z}(0) \qquad \tilde{z}(r) = \sum_{i=-1}^{n} w_i \cdot \phi(r - r_i)$$

where $r = r(x,y) = \sqrt{(x^2+y^2)}$, $r_i = \frac{i}{n}R$ and $w_{-1} = -\frac{\sum_{i=1}^{n} w_i \phi'(-r_i)}{\phi'(-r_{-1})}$. This ensures $z(0) = 0$ and $z'(0) = 0$.

The user chooses the basis function ϕ (see Fig. 1), the shape parameter s, the number of basis functions n, the weights w_i and the maximum radius R.

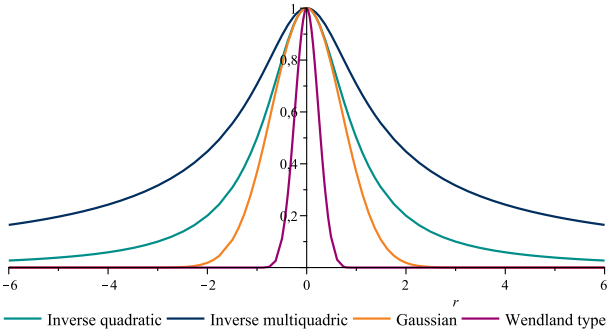

Fig. 1 *Plot of single basis functions with $s = 1$.*

$\phi(r)$	Basis function
$\frac{1}{1+(sr)^2}$	Inverse quadratic
$\frac{1}{\sqrt{1+(sr)^2}}$	Inverse multiquadric
$e^{-(sr)^2}$	Gaussian
$(1-sr)^6\left(\frac{35}{3}(sr)^2+6sr+1\right)$, $0 \le r \le \frac{1}{s}$	Wendland
0 , $\frac{1}{s} < r$	

3 Results

Systems used for evaluation are U.S. patents 5,636,065 (1st embodiment), 5,754,347 (2nd and 4th) and 6,028,713 (1st) with the aspheric surface replaced by a RBF surface; and a single mirror system with a field of 10.5 degrees. Variables set for optimization are the weights w_i for RBF surfaces, radii for spherical surfaces as well as radius and 3-5 polynomial coefficients for aspherical surfaces. Zemax is used for optimization.

3.1 Alternative representations

$z(0) = 0$ is ensured by $z(r) = \tilde{z}(r) - \tilde{z}(0)$. Alternatively, w_0 could be chosen appropriately. $z'(0) = 0$ is ensured by the choice of w_{-1}. Alternatively, w_1 could be chosen appropriately (and $i = -1$ omitted), or $z'(0) = 0$ could be completely forgone. Each of these alternatives leads in most cases to slightly inferior designs after optimization and in a lot of cases also to slower convergence during optimization.

3.2 Basis functions

The system performances after optimization of RBF surfaces with $n = 8$ basis functions is comparable to aspheres and shown in Fig. 2. No type of basis function performs significantly better than the others.

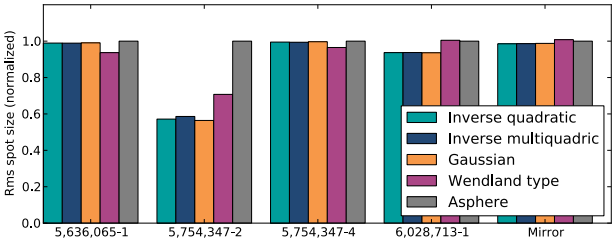

Fig. 2 *Performance of the different basis functions with $n = 8$ after optimization.*

3.3 Number of functions n

Increasing n from 4 to 16 reduces the rms spot size between 1,2% and 27,0% on the selected test cases as shown in Fig. 3.

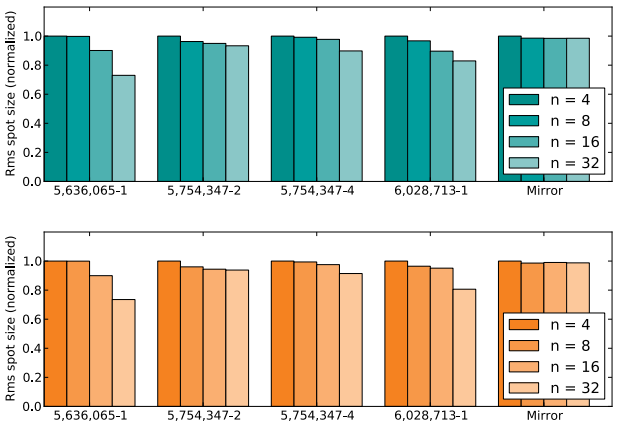

Fig. 3 *Normalized merit function values based on rms spot size for different values of n for inverse quadratic (top) and Gaussian (bottom).*

3.4 Shape parameter s

To compare values of s for different systems, we first observe that a form of scale invariance $\hat{z}(r) = \frac{z(\alpha r)}{\alpha}$ can be achieved by choosing $\hat{s} = \alpha s$, $\hat{w}_i = \frac{w_i}{\alpha}$ and $\hat{R} = \frac{R}{\alpha}$; in particular $\hat{R}\hat{s} = Rs$. For infinitely extended systems $\frac{sR}{n}$ remains constant under this scaling. Therefore we use $s^* = \frac{sR}{n}$ to identify suitable choices of s.

Fig. 4 shows an example of how the rms spot size after optimization depends on the value of s^*. Optimal values of s^* for the five test systems and $n \in \{4, 8, 16, 32\}$ are between 0.028 and 0.63 for the inverse quadratic and between 0.044 and 0.88 for the Gaussian.

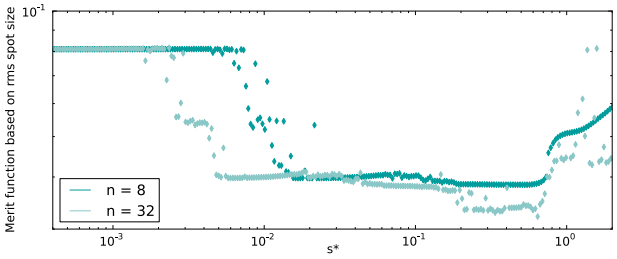

Fig. 4 *Merit functions values after optimization for different values of s^* with inverse quadratic on U.S. 6,028,713-1.*

3.5 Composition and locality

Fig. 5 shows different solutions for the first system. With different values of s, the way the surface is composed changes radically, while the rms spot sizes differ by no more than 11% for the pictured solutions. In general the values of s of good solutions also lead to single basis functions that are rather wide, so that a single weight w_i can influences a large region of the surface.

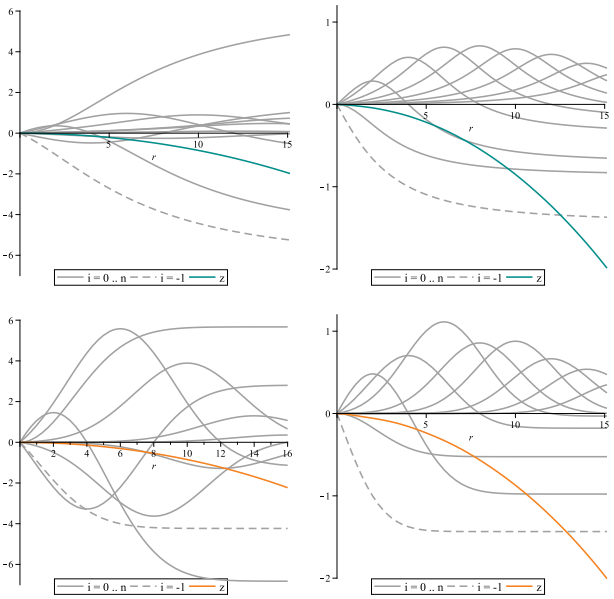

Fig. 5 *Composition of RBF surfaces for different solutions of the U.S. 5,636,065-1 system. Top: Inverse quadratic with $s^* = 0.2668$ (left) and $s^* = 0.6324$ (right). Bottom: Gaussian with $s^* = 0.44$ (left) and $s^* = 0.6324$ (right).*

4 Concluding remarks

Axially symmetric RBF surfaces provide a performance comparable to aspheres. Still, performance might be improved by using RBFs not to describe the complete surface but only the deviation from a base sphere or conic and by devising a strategy to deal with the shape parameter s during optimization.

As a single weight only influences a limited area of the surface, generalized non-symmetric RBF surfaces might enable more accurate modeling of off-axis surface areas.

Acknowledgments

The authors would like to thank the DFG and the TMBWK for the financial support through the projects “Verallgemeinerte optische Abbildungssysteme” (FKZ: HO 2667/1-1) and “Graduate Research School on Optical Microsystems Technology” (FKZ: 16SV5473).

References

[1] O. Cakmakci, K. Thompson, P. Vallee, J. Cote, and J. P. Rolland, “Design of a Freeform Single-Element Head-Worn Display,” in *Proceedings of SPIE*, vol. 7618 (2010).

[2] K.-H. Brenner, “Shifted Base Functions: An Efficient and Versatile New Tool in Optics,” in *Journal of Physics: Conference Series*, vol. 139 (2008).

[3] S. Ettl, J. Kaminski, M. C. Knauer, and G. Häusler, “Shape reconstruction from gradient data,” Applied Optics **47**(12), 2091–2097 (2008).